Caspase 9 is constitutively activated in mouse oocytes and plays a key role in oocyte elimination during meiotic prophase progression

Adriana C. Ene[1,*], **Stephanie Park**[1,*], **Winfried Edelmann**[2], and **Teruko Taketo**[1,3,**]

[1]Department of Biology, McGill University, Urology Research Laboratory, Royal Victoria Hospital, 687 Pine Avenue West, Montreal, Quebec H3A 1A1, Canada

[2]Department of Cell Biology, Albert Einstein College of Medicine, Bronx, NY, USA

[3]Department of Surgery, and Department of Obstetrics and Gynecology, McGill University, Urology Research Laboratory, Royal Victoria Hospital, 687 Pine Avenue West, Montreal, Quebec H3A 1A1, Canada

Abstract

In many mammalian species, more than half of the initial oocyte population is eliminated by neonatal life, thus limiting the oocyte reserve for reproduction. The cause or mechanism of this major oocyte loss remains poorly understood. We examined the apoptotic pathway involved in oocyte elimination in wild-type mouse ovaries as well as in *Msh5*–/– ovaries, in which all oocytes were eliminated due to a lack of double strand break repair. Immunoblot and immunofluorescence staining showed that an initiator caspase 9 and an effector caspase 7 were constitutively activated in almost all oocytes in fetal ovaries regardless of their genotypes. In caspase 9 –/– ovaries, the total number of oocytes remained high while that in wild-type ovaries steadily declined during ovarian development. Therefore, the activation of caspase 9 was required for but did not immediately lead to oocyte demise. We found that XIAP, an endogenous inhibitor of apoptosis, was also abundant in oocytes during meiotic prophase progression. On the other hand, a cleaved form of PARP1, a target of effector caspases, was localized to the nuclei of a limited number of oocytes, and the frequency of cleaved PARP1-positive oocyte nuclei increased significantly higher before all oocytes disappeared in *Msh5*–/– ovaries. We conclude that the mitochondrial apoptotic pathway mediated by caspase 9 is constitutively activated in oocytes and renders the elimination of oocytes with meiotic errors, which can be captured by the cleavage of PARP1.

Keywords

oocyte; apoptosis; caspase 9; Msh5; PARP1

**Correspondence: Teruko Taketo, Urology Research Laboratory, Royal Victoria Hospital, Room H6-19, 687 Pine Avenue West, Montreal, Quebec H3A 1A1, Tel: (514) 934-1934 x34197, Fax: (514) 843-1457, teruko.taketo@mcgill.ca..
*These authors equally contributed to this article

Introduction

Women are born with finite numbers of oocytes, thus limiting their reproductive life span. It is dogma that a female fetus starts with a large number of oocytes but loses as many as 70% of them before birth (Baker, 1963). The physiological role or cause of this massive oocyte loss remains unknown. A few hypotheses have been forwarded, mainly based on the studies in mice (reviewed by (Tilly, 2001)). One attractive hypothesis assumes that the oocytes with meiotic errors are eliminated by a checkpoint mechanism, contributing to the quality control of surviving oocytes. This hypothesis was originally proposed based on the morphological observations that a degeneration of oocytes is often seen around the pachytene stage, when homologous chromosomes complete pairing and recombination (Dietrich and Mulder, 1983; Beaumont and Mandl, 1962; Speed, 1988; Borum, 1961). This hypothesis was further supported by the findings that various mutations, which impair meiotic synapses or recombination, result in an excessive oocyte loss by the end of meiotic prophase progression (reviewed by (Cohen et al., 2006)). The pachytene checkpoint has been proposed in yeast and adapted to mammalian spermatogenesis (Ashley et al., 2004; Bailis and Roeder, 2000). However, it remains to be clarified how the checkpoint mechanism is activated in oocytes and leads to their demise.

Of three main mechanisms of cell death, necrosis, autophagy, and apoptosis, apoptosis has been implicated in oocyte death under physiological conditions although the role of autophagy has not yet been completely ruled out (de Felici, 2005; Morita and Tilly, 1999; Rodrigues et al., 2009). The signaling molecules involved in the apoptotic pathway of oocytes, particularly during meiotic prophase progression, remain to be identified. Two main apoptotic pathways, intrinsic and extrinsic pathways, are known to operate in mammalian cells (Thress et al., 1999; Los et al., 1999). The intrinsic pathway is triggered by various extracellular and intracellular stresses, such as growth factor withdrawal and DNA damage, and involves the release of cytochrome c from the mitochondria into the cytosol. The free cytochrome c binds to Apoptotic Protease-Activating Factor-1 (APAF-1), which then binds to an initiator caspase 9. The formation of this complex, named apoptosome, results in the activation of caspase 9 and the subsequent activation of effector caspases 3, 6, and/or 7. The active effector caspases in turn cleave a set of proteins, including poly-ADP ribose polymerase-1 (PARP1), causing the morphological changes typical of apoptosis. Caspase 2 has the molecular characteristics of an initiator caspase and can be activated by DNA damage upstream of the mitochondria pathway (Robertson et al., 2002). It can also be activated by other caspases (Slee et al., 1999). Members of the Bcl-2 family of proteins play a major role in governing the mitochondrial apoptotic pathway, with proteins such as Bad and Bax functioning as apoptosis inducers and Bcl-2 and Bcl-x as suppressors. The extrinsic pathway is activated by the binding of ligands such as Fas to death receptors on the cell membrane. This binding recruits a ligand-specific death domain, which in turn activates initiator caspase 8 or 10 and subsequent apoptotic events. The intrinsic and extrinsic pathways may cross talk to amplify apoptotic signals. For example, activated caspase 8 can initiate the mitochondrial apoptotic pathway by the cleavage of Bid. On the other hand, caspase 8 can also be activated downstream of caspase 9 (Kruidering M and Evan GI, 2000; Viswanath et al., 2001).

Targeted null mutations of apoptosis-related molecules provided important but incomplete information about oocyte loss. The deficiency in antiapoptotic molecules, Bcl-2 and Bcl-x, results in a marked reduction in the number of primordial follicles in neonatal ovaries (Ratts et al., 1995; Rucker et al., 2000). Furthermore, a null mutation of caspase 2 increases the number of primordial follicles (Flaws et al., 2001; Bergeron et al., 1998). On the other hand, no change was found when caspase 3, a key proapoptotic molecule, was absent (Matikainen et al., 2001). The consequence of Bax deficiency has been controversial; Perez et al. (Perez

et al., 1999) found no change, whereas we found a significant increase in the number of oocytes in neonatal ovaries (Alton and Taketo, 2007). Unfortunately, most above cases were examined only after birth. Since female germ cells are lost continuously while they go through mitosis and then various stages of meiotic prophase (McClellan et al., 2003), different apoptotic pathways may operate for the elimination of germ cells at different stages. Indeed, we have shown that oogonia are lost by a BAX-dependent apoptotic pathway whereas oocytes are lost during meiotic prophase progression in a BAX-independent mechanism (Alton and Taketo, 2007). Therefore, twice number of oocytes in the *Bax* deficient ovary after birth can be attributed to the suppression of the apoptotic death of oogonia, but not of oocytes. Thus, more studies are needed for clarifying the role of apoptosis in oocyte elimination.

In the present study, we examined the apoptotic pathway involved in the elimination of oocytes in fetal and neonatal wild-type mouse ovaries, as well as those deficient in *Msh5* as a model for meiotic errors. MSH5 is a member of the DNA mismatch repair protein family and plays a specific role in meiosis, in the repair of double strand breaks (DSBs) imposed at the onset of meiosis and in the consequent meiotic recombination (Edelmann et al., 1999). Therefore, in the absence of MSH5, DSBs remain unrepaired, resulting in excessive asynapses and oocyte loss (de Vries et al., 1999; Edelmann et al., 1999; Di Giacomo et al., 2005). We assumed that the excessive loss of oocytes with meiotic errors might reflect in changes of the apoptotic signaling pathway responsible for oocyte elimination.

Materials and Methods

Animals

All animal procedures were performed in accordance with the Canadian Council on Animal Care and approved by the McGill University Animal Care Committee. *Msh5* and *Casp9* null mutant carrier mice have been generated (Edelmann et al., 1999; Hakem et al., 1998) and maintained on the C57BL/6J (B6) genetic background in our mouse colony. B6 mice were purchased from the Jackson Laboratory (Bar Harbor, ME). Heterozygous mutant males and females were crossed to generate *Msh5* or *Casp9* wild-type (+/+), heterozygous mutant (+/ −), and homozygous mutant (−/−) progeny. The gestation age was defined as days postcoitum (dpc), assuming that copulation occurred at midnight. Delivery usually occurs at 19.5 dpc; however, we used dpc to specify postnatal ages for consistency. When ovaries were isolated, a piece of liver was also removed from each mouse, and used for genotyping by PCR amplification either directly (for *Msh5*) or after DNA isolation (for *Casp9*). PCR amplification included initial denaturation at 95°C for 10 min, 35 cycles of denaturation at 95°C for 30 sec, annealing at 55°C for 30 sec, and extension at 72°C for 1 min, followed by final extension at 72°C for 15 min using a thermocycler (Whatman Biometra, Goettingen, UK). The amplicons were analyzed by 2% agarose gel electrophoresis with ethidium bromide staining. Three primers, A, AGACCTGCACTGCGAGATCCG, B, TGGAAGGATTGGAGCTACGG, and C, TCTCGAATAGCCGTAGTCCCG were used for *Msh5* genotyping in early studies. The primers A and C amplified the wild type (approximately 300 bp) allele while the primers A and B amplified the mutant (approximately 400 bp) allele. However, these primers did not allow simultaneous amplification of both alleles due to sequence overlapping. Accordingly, we redesigned the primers A', AGGAGCCCGTGGTAGGAG and C', CCATGGATACAGGGAGAGTAATG to replace A and C in later studies. The results were consistent when both methods were applied to the same samples. For *Caps9* genotyping, we used primers CTTTGTCCCTCCTGTTGTGTCTTCA and CAGAGCGAGAATGAAGGGGAAACAA for detecting the wild-type allele (approximately 400 bp) and primers CTTATGTATTCCCGAGCCCGTGGTA and GTATGCTATACGAAGTTATTAGTCC for detecting the mutant allele (approximately 600 bp).

Histology preparations

Ovaries were isolated from fetuses or newborns, and fixed and embedded in paraffin as previously described (Taketo et al., 2005). Serial sections of 5 μm thickness were collected and used for IF staining.

Dissociated ovarian cell preparations

Immediately after isolation, ovaries without mesonephroi were dissociated, treated with a hypotonic solution (0.5 % NaCl, pH 8.2), and spun down onto histology slides as previously described (Alton and Taketo, 2007; Taketo, 2012). The slides were kept in a sealed box containing desiccators at −20°C until use.

Immunofluorescence (IF) staining

Ovarian sections on histology slides were deparaffinized and subjected to antigen retrieval as previously described (Taketo et al., 2005). Dissociated cell preparations on histology slides were directly processed for IF staining. All slides were incubated with primary antibodies overnight at either room temperature or 4°C, incubated with secondary antibodies conjugated with either biotin or fluorescence dyes, and incubated with avidin conjugated with fluorescence dyes of different color. Primary antibodies, secondary antibodies, and avidin-conjugates together with their sources and concentrations are given in Supplemental Table S1. The rat monoclonal antibody against GCNA1 and the mouse or rabbit polyclonal antibody against synaptonemal complex proteins (SC) were gifts from Drs. Enders (Enders and May, 1994) and P. Moens (Dobson et al., 1994), respectively. Other antibodies were purchased from AbCam (Cambridge, MA), Santa Cruz Biotechnology (Santa Cruz, CA), Cell Signaling Technology (Danvers, MA), Imgenex (San Diego, CA), Pierce Endogen (Rockford, IL), Novus Biologicals (Littleton, CO), Vector (Burlingame, CA), and Molecular Probes (Eugene, OR). After IF staining, the slides were air-dried and mounted in the Prolong Antifade mounting medium (Molecular Probe) containing 1.0 μg/ml 4',6-diamidin-2'-phenylindole dihydrochloride (DAPI) (Roche Diagnostics, Mannheim, Germany). Fluorescent signals were examined under an epifluorescence microscope (Zeiss Axiophot, Germany). All images were captured with a digital camera (Retiga 1300, QImaging, Burnaby, BC) and processed with Northern Eclipse digital imaging software, version 6.0 (Empix Imaging, Mississauga, ON). No distinct signals were seen when the primary antibodies were omitted (negative control).

Immunoblot

All chemicals and equipment for electrophoresis and transfer were purchased from Bio-Rad (Mississauga, ON) unless specified. Each pair of fetal ovaries was snap-frozen in a microfuge tube and stored at −80°C. Each sample was lysed in 15 or 20 μl sample buffer containing dithiothreitol by repeating freezing and thawing until no more tissue chunks were visible, followed by boiling for 10 min, vortex-mixing, and centrifugation. Some ovaries were stored in sample buffer at −80°C before lysis. The supernatant of each sample and a broad-range biotinylated molecular weight standard mix as well as controls (Jurkat cells with or without treatment with etoposide, Cell Signaling Technology) were loaded on 15% or 4–15% gradient bis-polyacrylamide gel containing SDS. The proteins after fractionation in SDS-PAGE were transferred electrophoretically to 0.45 μm nitrocellulose membranes in Tris-glycine buffer containing 20% methanol by using a Trans-Blot Cell apparatus. The membranes were blocked with 5% skim milk and incubated with the primary antibody, followed by the secondary antibody conjugated with biotin. The primary antibodies used, their sources, and concentrations are given in Supplemental Table S1. The membranes were then incubated with a donkey anti-rabbit antibody conjugated with biotin (Jackson ImmunoResearch, Mississauga, OT) at 1:5.000 dilutions, followed by a goat anti-biotin

antibody conjugated with horseradish peroxidase (HRP) at 1:500 dilutions. The enzymatic activity of HRP was detected with Lumi-Light ECL kit (Roche Diagnostics). The bands were digitized by using an Agfa Snapscan 1236 scanner (Agfa-Gevaert, NV) and analyzed with the Un-Scan-It gel software version 5.1 (Silk Scientific, Orem. UT).

RT-PCR

Total RNA was isolated from each ovary using the microRNeasy kit (Quiagen, Mississauga, ON) including DNase I digestion and eluted in 14 μl water, 10 μl of which was subjected to first strand cDNA synthesis with random hexamers and Superscript III according to the manufacturer's instruction (Invitrogen Life Technologies, Burlington, ON). *cIAP1, cIAP2, XIAP*, and *Survivin* were amplified by adding 2 μl cDNA aliquot and primers in a total 50 μl reaction mixture as previously reported (Kawamura et al., 2003) for 30 cycles.

Statistical analyses

The total number of germ cells was counted in each ovary from at least three females and two litters, unless specified, and the mean and standard errors of the mean (SEM) was calculated in each group. The percentages of meiotic substages were estimated by counting over 100 GCNA1-positive cells per ovary. For double staining of GCNA1 and cPARP1 in each dissociated cell preparation, at least 100 GCNA1-positive cells were identified and its staining with cPARP1 was recorded. Only those with GCNA1 and DAPI staining were considered as oocyte nuclei. Immnoblots were repeated starting from separate pairs of ovaries. Significant difference between groups was estimated by student's t-test, ANOVA, or regression analysis.

Results

The loss of germ cells in fetal and neonatal *Msh5* mutant ovaries

We first compared the changes in the total number of germ cells (i.e., oogonia and oocytes) between *Msh5* +/+, +/−, and −/− ovaries during development. We identified the germ cells in dissociated cell preparations of each ovary by IF staining for GCNA1 (Enders and May, 1994). The numbers of GCNA1-positive cells in *Msh5* +/+ and +/− ovaries were not different and pooled as the control. The numbers in *Msh5* −/− ovaries were consistently lower than those in the control ovaries from 17.5 dpc onwards, but reached significant differences (P<0.05) at 19.5 and 20.5 dpc (Fig. 1). The overall rate of germ cell loss (i.e., the slope) was similar between *Msh5* −/− and the control ovaries. We did not count the number of germ cells beyond 20.5 dpc because GCNA1 expression ceased at mid diplotene stage (Alton & Taketo, 2006). We confirmed that very few germ cells were identified by IF staining for Mouse Vasa Homolog (MVH), a cytoplasmic maker for germ cells (Toyooka et al., 2000), in the histological sections of *Msh5* −/− ovaries at 22.5 dpc (not shown).

Meiotic prophase progression in *Msh5 −/−* ovaries

Next, we compared meiotic prophase progression in the dissociated cell preparations of *Msh5* −/− and the control ovaries by double IF staining for SC and γ-H2AX (Fig. 2A). We introduced IF staining for γ-H2AX because the zygotene and early diplotene stages or the leptotene and late diplotene stages were often difficult to distinguish by SC staining alone. In the control ovaries, γ-H2AX staining was seen in the entire nucleus at the leptotene and zygotene stages and largely disappeared by the mid pachytene stage (Fig. 2Aa–g). γ-H2AX staining remained in several foci in some early pachytene oocytes or along one or a few SC cores, probably associated with persistent asynapses, in pachytene and diplotene oocytes (Fig. 2Ad); however, these staining patterns were distinct from those in zygotene oocytes. According to these criteria, the meiotic prophase was found to have progressed steadily from

the zygotene to diplotene stage in the control ovaries from 16.5 to 20.5 dpc (Fig. 2B). These definitions of meiotic prophase stages could not simply be applied to *Msh5* −/− ovaries. Typical leptotene and zygotene oocytes were observed (Fig. 2Ah & i). However, based on the above definition, the majority of oocytes remained at the zygotene stage, showing incomplete synapses and heavy γ-H2AX staining, from 16.5 through 20.5 dpc (Fig. 2Aj & k). These oocytes could have been at the pachytene stage with extensive asynapses or the diplotene stage with persistent γ-H2AX staining. A small number of oocytes appeared to be pachytene with faint or no γ-H2AX staining; but they all had excessive number of SC cores (not shown).

Cleavage of caspases detected by immunoblots of ovaries

To identify the apoptotic pathway involved in oocyte elimination, we examined the cleavage (activation) of various caspases in *Msh5* +/+ and −/− ovaries at 16.5–19.5 dpc by immunoblots (Fig. 3). The results indicated a robust increase in the activation of caspase 9 with a peak at 18.5 dpc in both genotypes of ovaries. The antibody from Cell Signaling detected the procaspase 9 at 49 kDa and its cleaved forms at 37 and 39 kDa (Fig. 3A). We calculated the ratio of band intensities at 37 kDa vs. 49 kDa in each lane as the activation level, which reached about 1:1 on average at 18.5 dpc. The antibody from Imgenex detected only the cleaved forms at 15 and 35 kDa (Fig. 3A) and, therefore, could not be used for the calculation of activation levels, although results were comparable to the detection of the 37 kDa fragment. By contrast, the activation of caspases 7 (Fig. 3B), 2 and 6 (not shown) remained minimal and that of caspase 3 was undetectable although their full forms were easily detectable at all examined stages. No significant difference in the activation levels was found between *Msh5* +/+ and −/− ovaries for all caspases and developmental stages examined.

IF localization of cleaved caspases in ovarian sections

Excessive activation of apoptotic pathway in *Msh5* −/− oocytes, even if it occurred, might not have been reflected into the immunoblot of entire ovaries. To examine the activation of caspases in the oocyte, we performed IF staining of ovarian sections with the antibody which specifically recognized the cleaved forms of caspase 9. With the antibody from Imgenex, homogeneous fluorescence staining was seen in the cytoplasm of almost all oocytes in *Msh5* +/+ ovaries at 16.5 dpc (Fig. 4a & b). At 18.5 dpc, the intensity of IF staining increased in some oocytes while it decreased in others (Fig. 4c & d). Faint IF staining was visible in somatic cells near oocytes but was absent in the area devoid of oocytes. Similar localization of cleaved caspase 9 was seen with the antibody from Cell Signaling or in *Msh5* −/− ovaries (not shown). IF staining with the antibody which recognized the 20 kDa fragment of caspase 7 also showed a similar localization to cleaved caspase 9 in *Msh5* +/+ ovaries (Fig. S1), as well as in *Msh5* −/− ovaries (not shown). No remarkable IF staining was seen with the antibody which recognized the 17/19 kDa fragments of caspase 3 (not shown). The negative control without primary antibodies did not show IF staining over the background level.

Oocyte retention in Caspase 9 −/− ovaries

To test whether activation of caspase 9 plays a role in oocyte elimination, we examined the total number of GCNA1-positive cells in Caspase 9 (*Casp9*) +/+, +/−, and −/− ovaries at 16.5–19.5 dpc. As previously reported, the survival of Casp9 −/− fetuses decreased rapidly during this period (Hakem et al., 1998; Kuida et al., 1998). Nonetheless, we obtained a small number of *Casp9* −/− female progeny up to 19.5 dpc. The number of GCNA1-positive cells in *Casp9* −/− ovaries was comparable with that in *Casp9* +/+ ovaries at 16.5 and 18.5 dpc (Fig. 5A). However, the overall loss of oocytes during ovarian development in *Casp9*−/− ovaries from 16.5 to 19.5 dpc (r = −0.34552) was much slower than that in *Casp9* +/+

ovaries (r = −0.95378) with a significant difference (p<0.001) (Fig. 5B). Consequently, the total number of GCNA1-positive cells in *Casp9* −/− ovaries became twice as large as that in *Casp9* +/+ ovaries at 19.5 dpc (Fig. 5A).

Next, we examined at which stage the excessive number of oocytes were accumulated in *Casp9* −/− ovaries. According to double staining of GCNA1 and SC in dissociated ovarian cells, typical zygotene and pachytene oocytes were seen at 16.5 and 18.5 dpc, and the vast majority were at the diplotene-like stage at 19.5 dpc (not shown). However, we could not rule out the possibility that the latter cells were actually at the leptotene or early zygotene stages by SC staining alone. To verify meiotic progression in *Casp9* −/− ovaries, we performed IF staining for GCNA1 and γH2AX in ovarian sections (Fig. 6). Most oocytes in both *Casp9* +/+ and −/− ovaries were at the late leptotene to mid zygotene stages with heavy γH2AX staining at 16.5 dpc (Fig. 6a–d), and progressed to the pachytene stage with fine γH2AX foci at 18.5 dpc (Fig.6e–h). At 19.5 dpc, the number of GCNA1-positive cells were visibly greater in *Casp9* −/− ovaries than Casp9 +/+ ovaries (Fig. 6i–l). Many GCNA1-positive cells were γH2AX-negative, a characteristic of the late meiotic prophase, in both genotypes of ovaries. Thus, the oocytes appeared to have progressed through the meiotic prophase and were accumulated at the end of the meiotic prophase in *Casp9* −/− ovaries.

Expression and localization of IAPs in ovaries

In the presence of constitutively activated caspases, oocytes must be protected from apoptotic demise. We speculated that one or more of endogenous Inhibitor of Apoptosis Proteins (IAPs) may have counterbalanced the activity of caspases and allowed for the survival of oocytes. We confirmed that cIAP1, cIAP2, XIAP, and Survivin were expressed in *Msh5* +/+ ovaries at 18.5 dpc by RT-PCR (not shown). IF staining showed that XIAP was abundant in the cytoplasm of almost all oocytes in both *Msh5* +/+ and −/− ovaries at 16.5 dpc (Fig. 7a & b). The staining for XIAP was intensified and occasionally seen in the nuclei of some oocytes in *Msh5* +/+ ovaries at later stages (Fig. 7c). On the other hand, the intensity of IF staining was considerably reduced in *Msh5* −/− ovaries at 19.5 dpc (Fig. 7d).

Localization of cleaved PARP1 in ovaries

Since the activation of caspases is constitutive and cannot be used for indicating the oocytes undergoing apoptotic demise, we searched for their downstream apoptotic markers. TUNEL detects DNA fragmentation, one of the final apoptotic events, and is often used as an apoptosis indicator. However, TUNEL does not correspond to oocyte demise during meiotic prophase progression for unknown reason (de Felici et al., 2008; Ghafari et al., 2007; Pepling and Spradling, 2001)(our unpublished observation). On the other hand, the cleavage of PARP1 has been shown to be associated with oocyte elimination during cyst breakdown in neonatal ovaries (Pepling and Spradling, 2001). Hence, we examined the localization of cleaved PARP1 (cPARP1) with the antibody which recognized its 24 kDa fragment in ovarian sections. The IF staining was restricted to the nuclei of a few oocytes per section from both *Msh5* +/+ and −/− ovaries at 16.5–18.5 dpc (not shown). The frequency of cPARP1-positive cells increased in *Msh5* +/+ ovaries and more so in *Msh5* −/− ovaries at 19.5 dpc (Fig. 8). We performed immunoblot of ovarian homogenate with an antibody against the full-form of PARP1. The cleavage of PARP1 was detectable at all stages and no difference was found between *Msh5* +/+ and −/− ovaries (not shown).

Frequency of cPARP1-positive oocytes

To test whether the cleavage of PARP1 represents the apoptosis execution in oocytes, we compared the frequency of cPARP1-positive oocytes in *Msh5* −/− and the control ovaries by double staining for GCNA1 and cPARP1 in dissociated cell preparations. Under an epi-fluorescence microscope, more than 100 GCNA1-positive nuclei were identified per ovary,

and their staining for cPARP1 was recorded. Only those with DAPI staining were considered to be oocyte nuclei. Various staining patterns were observed in both *Msh5* +/+ and −/− ovaries (Fig. 9A). Most of GCNA1-positive cells were negative for cPARP1. Some oocytes had typical nuclear sizes and were fully labeled for cPARP1 (Fig. 9Aa & b) whereas some nuclei were partially covered by GCNA1 staining and fully covered by cPARP staining (Fig. 9Ac). The dominant staining pattern was the GCNA1-positive nuclei with intense cPARP1 staining but of much smaller sizes compared to typical oocyte nuclei (Fig. 9Ad). Many cells were found to be negative for GCNA1 and positive for cPARP1 (Fig. 9Ae). Since these cell types could not be identified, they were not included for counting. As summarized in Fig. 9B, the percentage of cPARP1-positive oocytes was about 10% in the ovaries of all three genotypes at 16.5 – 19.5 dpc, and increased to about 20% in both *Msh5* +/+ and +/− ovaries and 60% (P<0.01) in *Msh5* −/− ovaries at 20.5 dpc. It decreased to the basal line in *Msh5* +/+ and +/− ovaries but remained significantly higher (P<0.05) in *Msh5* −/− ovaries at 21.5 dpc. Thus, the frequency of c PARP1-positive oocyte nuclei increased preceding the loss of all oocytes in *Msh5* −/− ovaries.

Discussions

The meiotic prophase in the oocyte is a critical period for female fertility. Proper pairing and recombination between homologous chromosomes determines the success in chromosome segregation at the first meiotic division and subsequent embryonic development. Furthermore, a major elimination of oocytes occurs during this period to limit the oocyte reserve for reproduction. If selection takes place in oocyte elimination, this event also influences the quality of oocytes in reserve. Despite its importance, neither the cause nor the regulatory mechanism of physiological oocyte elimination is well understood. Our current studies show that the mitochondrial apoptotic pathway mediated by caspase 9 plays a role in oocyte demise during meiotic prophase progression. However, caspase 9, and caspase 7 to a lesser extent, are constitutively activated in all oocytes and, therefore, do not immediately lead to oocyte demise. We speculate that the endogenous apoptosis inhibitors, particularly XIAP, may counterbalance the activity of caspases and allow for the oocytes to survive. We further show that the cleavage of PARP1 is, so far, the best indicator of apoptotic execution in the oocytes during meiotic prophase progression.

Constitutive activation of caspase 9 in *Msh5* +/+ and −/− ovaries

Our results indicate that caspase 9 is constitutively activated in the oocytes during meiotic prophase progression as demonstrated by IF staining of cleaved caspase 9. Consequently, the fate of oocytes must be regulated in its downstream mechanisms. Caspase 7 appears to be a stronger candidate of the effector caspase downstream of caspase 9 than caspase 3. This conclusion is consistent with the report that a caspase 3 null mutation does not affect the number of follicles in neonatal ovaries (Matikainen et al., 2001). However, while immunoblot of entire ovaries demonstrated a robust increase in the activation of caspase 9 with a peak at 18.5 dpc, none of the effector caspases showed activation levels comparable to that of caspase 9. We speculate that the proteolytic activity of caspase 9 was suppressed by cIAPs and, therefore, its downstream caspase activation was not as robust as caspase 9 activation.

Essential role of caspase 9 in the elimination of oocytes

A role of caspase 2 and mitochondrial anti-apoptotic components Bcl-2 and Bcl-x in the regulation of oocyte population in fetal life has been previously reported (Flaws et al., 2001; Ratts et al., 1995; Rucker et al., 2000). However, no evidence was provided for their roles specifically in the elimination of oocytes during meiotic prophase progression. We have revealed that a mitochondrial pro-apoptotic component Bax is required for the elimination of

oogonia but not that of oocytes (Alton and Taketo, 2007). In the present study, we have shown that the mitochondrial apoptotic pathway mediated by caspase 9 is indeed required for the elimination of oocytes in the meiotic prophase. The total number of germ cells did not differ with or without the caspase 9 deficiency at 16.5 or 18.5 dpc, but reached significantly higher levels with caspase 9 deficiency at 19.5 dpc, at which stage the majority of oocytes had completed homologous chromosome pairing and recombination. Furthermore, the rate of oocyte loss was much slower in *Casp9* −/− ovaries than in *Casp9* +/+ or +/− ovaries from 16.5 dpc to 19.5 dpc. Therefore, we speculate that caspase 9 is particularly important for the elimination of oocytes with meiotic errors such as asynapsis. It will be interesting to examine the surviving oocytes in *Casp9* −/− ovaries at later stages. Unfortunately, most *Casp9* −/− progeny die perinatally. A conditional knockout of caspase 9 in the oocyte would be useful for further studies.

Possible protection of oocytes by XIAP from apoptotic elimination

In the presence of constitutively active caspases, oocytes must be protected from apoptotic elimination to survive. Such protection may be provided by cIAPs, endogenous apoptosis inhibitors. Eight cIAP family proteins have been identified in mammals. Of these, cIAP1 (HIAP), cIAP2 (HIAP2), and XIAP are known to bind and potently inhibit caspases 3, 7, and 9, but not caspase 1, 6, or 8 (Deveraux et al., 1997; Deveraux et al., 1998). Furthermore, these cIAP1s possess an E3 ubiquitin ligase activity, suggesting that the degradation of caspases may be another mechanism by which cIAPs suppress apoptosis (Conze et al., 2005; Vaux and Silke, 2005). In the present study, we confirmed that cIAP1, cIAP2, and XIAP were transcribed in *Msh5* +/+ ovaries. Furthermore, XIAP, known to be the most potent cIAP, was localized to the cytoplasm of almost all oocytes in ovaries at 16.5 dpc and decreased in IF staining intensity, particularly in *Msh5* −/− ovaries, at 19.5–20.5 dpc. This window may have allowed for the apoptotic elimination of oocytes with meiotic errors. Alternatively, meiotic errors may result in the reduction of XIAP levels and consequent apoptotic elimination. A similar role of XIAP has been suggested for the survival of granulosa and Sertoli cells, in which caspases are constitutively activated (Johnson et al., 2008; Li et al., 1998). On the other hand, an *Xiap* −/− mutant mouse has been reported to be healthy and fertile (Harlin et al., 2001); however, the redundancy among cIAP1s is a concern. Oocyte-specific overexpression of XIAP may address the role of XIAP in oocyte elimination.

Nuclear localization of cleaved PARP1 captures the oocytes undergoing apoptotic demise

In contrast to the ubiquitous presence of cleaved caspases in oocytes, cPARP1 was localized to the nuclei of a small number of oocytes in ovarian sections. In dissociated ovarian cells, the percentage of cPARP1-positive oocytes was steady at around 10% in the ovaries of all three genotypes and transiently increased in *Msh5* +/+ and +/− ovaries at 20.5 dpc. Ghafari et al. (Ghafari et al., 2007) have reported that 10–50% of oocytes are positive for cPARP1 at all stages during meiotic prophase progression in normal mouse ovaries. In our studies, however, 20% was the maximum frequency of cPARP1-positive oocytes in the control ovaries. In contrast, the percentage of cPARP1-positive oocytes in *Msh5* −/− ovaries increased to 60% at 20.5 dpc and remained higher at 21.5 dpc. Since most oocytes were eliminated in *Msh5* −/− ovaries by 22.5 dpc, the high frequency of cPARP1 appeared to precede the oocyte loss. Some cPARP1-positive nuclei had the size and shape comparable to those of cPARP1-negative nuclei, indicating that the cleavage of PARP1 is one of the earliest events in the oocytes undergoing apoptotic demise. However, the majority of nuclei labeled for both GCNA1 and cPARP1 were much smaller in size than typical oocyte nuclei and many more nuclei were positive for cPARP1 and negative for GCNA1. We speculate that once an oocyte was committed to apoptotic elimination, its nucleus rapidly became picnotic while GCNA1 was degraded.

Summary

We have previously reported steady oocyte loss from 13.5 to 21.5 dpc in normal mouse ovaries (McCllelan et al., 2003). Since a caspase 9 deficiency did not influence the oocyte population up to 18.5 dpc, the early phase of oocyte elimination may not involve the mitochondiral apoptotic pathway. The extrinsic apoptotic pathway or autophagy may play a role in oocyte loss in this phase. By contrast, the later phase of oocyte loss was prevented and the total number of oocytes became significantly greater in *Casp9* −/− ovaries at 19.5 dpc. On the other hand, the total number of oocytes was significantly decreased in *Msh5* −/− ovaries at 19.5 dpc. Furthermore, the percentage of cPARP1 oocytes in *Msh5* −/− ovaries dramatically increased to higher levels than the control ovaries at 20.5 and 21.5 dpc, soon before complete loss of oocytes. These results suggest that the caspase 9-dependent apoptotic pathway operates specifically for the elimination of oocytes with meiotic errors during a narrow window between 18.5 and 21.5 dpc. Two major questions remain to be addressed: what triggers the apoptotic execution of oocytes in normal ovaries; and what inhibits the cIAP activity to allow for oocyte demise.

Supplementary Material

Refer to Web version on PubMed Central for supplementary material.

Acknowledgments

References

Alton M, Taketo T. Switch from BAX-dependent to BAX-independent germ cell loss during the development of fetal mouse ovaries. J Cell Sci. 2007; 120:417–424. [PubMed: 17213335]

Ashley T, Westphal C, de Maggio AP, de Rooij DG. The mammalian mid-pachytene checkpoint: meiotic arrest in spermatocytes with a mutation in Atm alone or in combination with a Trp53(P53) or Cdkn1a (P21/cip1) mutation. Cytogenet Genome Res. 2004; 107:256–262. [PubMed: 15467370]

Bailis JM, Roeder GS. Pachytene exit controlled by reversal of Mek1-dependent phosphorylation. Cell. 2000; 101:211–221. [PubMed: 10786836]

Baker TG. A quantitative and cytological study of germ cells in human ovaries. Proc. R. Soc. Lond. 1963; B158:417–433. [PubMed: 14070052]

Beaumont HM, Mandl AM. A quantitative and cytological study of oogonia and oocytes in the foetal and neonatal rat. Proc. R. Soc. Lond. 1962; B155:557–579.

Bergeron L, Perez GI, Macdonald G, Shi L, Sun Y, Jurisicova A, Varmuza S, Latham KE, Flaws JA, Salter JCM, Hara H, Moskowitz MA, Li E, Greenberg A, Tilly JL, Yuan J. Defects in regulation of apoptosis in caspase-2-deficient mice. Genes Dev. 1998; 12:1304–1314. [PubMed: 9573047]

Borum K. Oogenesis in the mouse. A study of the meiotic prophase. Exp Cell Res. 1961; 24:495–507. [PubMed: 13871511]

Cohen PE, Pollack SE, Pollard JW. Genetic analysis of chromosome pairing, recombination, and cell cycle control during first meiotic prophase in mammals. Endocr Rev. 2006; 27:398–426. [PubMed: 16543383]

Conze DB, Albert L, Ferrick DA, Goeddel DV, Yeh W-C, Mak T, Ashwell JD. Posttranscriptional downregulation of c-IAP2 by the ubiquitin protein ligase c-IAP1 in vivo. Mol. Cell. Biol. 2005; 25:3348–3356. [PubMed: 15798218]

de Felici M. Establishment of oocyte population in the fetal ovary: primordial germ cell proliferation and oocyte programmed cell death. RBM Online. 2005; 10:182–191. [PubMed: 15823221]

de Felici M, Lobascio AM, Klinger FG. Cell death in fetal oocytes. Autophagy. 2008; 4:240–242. [PubMed: 18094606]

de Vries SS, Baart EB, Dekker M, Siezen A, de Rooij DG, de Boer P, te Riele H. Mouse MutS-like protein Msh5 is required for proper chromosome synapsis in male and female meiosis. Genes Dev. 1999; 13:523–531. [PubMed: 10072381]

Deveraux QL, Roy N, Stennicke HR, van Arsdale T, Zhou Q, Srinivascula SM, Alnemri ES, Salvesen GS, Reed JC. IAPs block apoptotic events induced by caspase-8 and cytochrome c by direct inhibition of distinct caspases. EMBO J. 1998; 17:2215–2223. [PubMed: 9545235]

Deveraux QL, Takahashi R, Salvesen GS, Reed JC. X-linked IAP is a direct inhibitor of cell-death proteases. Nature. 1997; 388:300–303. [PubMed: 9230442]

Di Giacomo M, Barchi M, Baudat F, Edelmann W, Keeney S, Jasin M. Distinct DNA-damage-dependent and -independent responses drive the loss of oocytes in recombination-defective mouse mutants. Proc. Natl. Acad. Sci. USA. 2005; 102:737–742. [PubMed: 15640358]

Dietrich AJJ, Mulder RJP. A light and electron microscopic analysis of meiotic prophase in female mice. Chromosoma. 1983; 88:377–385. [PubMed: 6197255]

Dobson MJ, Pearlman RE, Karaiskakis A, Spyropoulos B, Moens PB. Synaptonemal complex proteins: occurrence, epitope mapping and chromosome disjunction. J. Cell Sci. 1994; 107:2749–2760. [PubMed: 7876343]

Edelmann W, Cohen PE, Kneitz B, Winand N, Lia M, Heyer J, Kolodner R, Pollard JW, Kucherlapati R. Mammalian Mut5 homologue 5 is required for chromosome pairing in meiosis. Nature Genet. 1999; 21:123–127. [PubMed: 9916805]

Enders GC, May JJI. Developmentally regulated expression of a mouse germ cell nuclear antigen examined from embryonic Day 11 to adult in male and female mice. Dev. Biol. 1994; 163:331–340. [PubMed: 8200475]

Flaws JA, Hirshfield AN, Hewitt JA, Babus JK, Furth PA. Effect of Bcl-2 on the primordial follicle endowment in the mouse ovary. Biol. Reprod. 2001; 64:1153–1159. [PubMed: 11259262]

Ghafari F, Gutierrez CG, Hartshorne GM. Apoptosis in mouse fetal and neonatal oocytes during meiotic prophase one. BMC Dev. Biol. 2007; 7:87. [PubMed: 17650311]

Hakem R, Hakem A, Duncan GS, Henderson JT, Woo M, Soengas MS, Elia A, de la Pompa JL, Kagi D, Khoo W, Potter J, Yoshida R, Kaufman SA, Lowe SW, Penninger JM, Mak TW. Differential requirement for caspase 9 in apoptotic pathways in vivo. Cell. 1998; 94:339–352. [PubMed: 9708736]

Harlin H, Reffey SB, Duckett CS, Lindsten T, Thompson CB. Characterization of XIAP-deficient mice. Mol. Cell. Biol. 2001; 21:3604–3608. [PubMed: 11313486]

Johnson C, Jia Y, Wang C, Lue Y-H, Swerdloff RS, Zhang X-S, Hu Z-Y, Li Y-C, Liu Y-X, Hikim APS. Role of caspase 2 in apoptotic signaling in primate and murine germ cells. Biol. Reprod. 2008; 79:806–814. [PubMed: 18614702]

Kawamura K, Sato N, Fukuda J, Kodama H, Kumagai J, Tanikawa H, Shimizu Y, Tanaka T. Survivin acts as an antiapoptotic factor during the development of mouse preimplantation embryos. Dev. Biol. 2003; 256:331–341. [PubMed: 12679106]

Kruidering M, Evan GI. Caspase-8 in apoptosis: The beginning of 'the end'? IUBMB Life. 2000; 50:85–90. [PubMed: 11185963]

Kuida K, Haydar TF, Kuan C-Y, Gu Y, Taya C, Karasuyama H, Su MSS, Rakic P, Flavell RA. Reduced apoptosis and cytochrome c - mediated caspase activation in mice lacking caspase 9. Cell. 1998; 94:325–337. [PubMed: 9708735]

Li J, Kim J-M, Liston P, Li M, Miyazaki T, Mackenzie AE, Korneluk RG, Tsang BK. Expression of inhibitor of apoptosis proteins (IAPs) in rat granulosa cells during ovarian follicular development and atresia. Endocrinology. 1998; 139:1321–1328. [PubMed: 9492068]

Los M, Wesselborg S, Schulze-Osthoff K. The role of caspases in development, immunity, and apoptotic signal transduction: Lessons from knockout mice. Immunity. 1999; 10:629–639. [PubMed: 10403638]

Matikainen T, Perez GI, Zheng TS, Kluzak TR, Rueda BR, Flavell RA, Tilly JL. Caspase-3 gene knockout defines cell lineage specificity for programmed cell death signaling in the ovary. Endocrinology. 2001; 142:2468–2479. [PubMed: 11356696]

McClellan KA, Gosden R, Taketo T. Continuous loss of oocytes throughout meiotic prophase in the normal mouse ovary. Dev. Biol. 2003; 258:334–348. [PubMed: 12798292]

Morita Y, Tilly JL. Oocyte apoptosis: Like sand through an hourglass. Dev. Biol. 1999; 213:1–17. [PubMed: 10452843]

Pepling ME, Spradling AC. Mouse ovarian germ cell cysts undergo programmed breakdown to form primordial follicles. Dev. Biol. 2001; 234:339–351. [PubMed: 11397004]

Perez GI, Robles R, Knudson CM, Flaws JA, Korsmeyer SJ, Tilly JL. Prolongation of ovarian lifespan into advanced chronological age by Bax-deficiency. Nature Genet. 1999; 21:200–203. [PubMed: 9988273]

Ratts V, Flaws JA, Kolp R, Sorenson CM, Tilly JL. Ablation of bcl-2 gene expression decreases the numbers of oocytes and primordial follicles established in the post-natal female mouse gonad. Endocrinology. 1995; 136:3665–3668. [PubMed: 7628407]

Robertson JD, Enoksson M, Suomela M, Zhivotovsky B, Orrenius S. Caspase-2 acts upstream of mitochondria to promote cytochrome c release during etoposide-induced apoptosis. J. Biol. Chem. 2002; 277:29803–29809. [PubMed: 12065594]

Rodrigues P, Limback D, McGinnis LK, Plancha CE, Albertini DF. Multiple mechanisms of germ cell loss in the perinatal mouse ovary. Reproduction. 2009; 137:709–720. [PubMed: 19176312]

Rucker EBI, Dierisseau P, Wagner K-U, Garrett L, Wynshaw-Boris A, Flaws JA, Hennighausen L. Bcl-x and Bax regulate mouse primordial germ cell survival and apoptosis during embryogenesis. Mol. Endocrinol. 2000; 14:1038–1052. [PubMed: 10894153]

Slee EA, Harte MT, Kluck RM, Wolf BB, Casiano CA, Newmeyer DD, Wang H-G, Reed JC, Nicholson DW, Alnemri ES, Green DR, Martin SJ. Ordering the cytochrome c-initiated caspase cascade: hierarchical activation of caspases-2, -3, -6, -7, -8, and -10 in a caspase-9-dependent manner. J. Cell Biol. 1999; 144:281–292. [PubMed: 9922454]

Speed RM. The possible role of meiotic pairing anomalies in the atresia of human fetal oocytes. Hum. Genet. 1988; 78:260–266. [PubMed: 3346015]

Taketo T. Microspread oocyte preparations for the analysis of meiotic prophase progression with improved recovery by cytospin centrifugation. Methods Mol.r Biol. 2012; 825:173–181.

Taketo T, Lee C-H, Zhang J, Li Y, Lee C-YG, Lau Y-FC. Expression of SRY proteins in both normal and sex-reversed XY fetal mouse gonads. Dev. Dyn. 2005; 233:612–622. [PubMed: 15789443]

Thress K, Kornbluth S, Smith JJ. Mitochondria at the crossroad of apoptotic cell death. J. Bioenerget. Biomembr. 1999; 31:321–326.

Tilly JL. Commuting the death sentence: How oocytes strive to survive. Nature Rev. Mol. Cell Biol. 2001; 2:838–848. [PubMed: 11715050]

Toyooka Y, Tsunekawa N, Takahashi Y, Matsui Y, Satoh M, Noce T. Expression and intracellular localization of mouse Vasa-homologue protein during germ cell development. Mech. Dev. 2000; 93:139–149. [PubMed: 10781947]

Vaux DL, Silke J. IAPs - the ubiquitin connection. Cell Death Diff. 2005; 12:1205–1207.

Viswanath V, Wu Y, Boonplueang R, Chen S, Stevenson FF, Yantiri F, Yang L, Flint BM, Andersen JK. Caspase-9 activation results in downstream caspase-8 activation and bid cleavage in 1-methyl-4-phenyl-1,2,3,6-tetrahydropyridine-induced Parkinson's disease. J Neurosci. 2001; 21:9519–9528. [PubMed: 11739563]

Highlights

- To indicate that the apoptotic pathway is constitutively activated in the mouse oocyte.

- To provide evidence that caspase 9 is essential for the elimination of oocytes during meiotic prophase progression.

- To provide evidence that cleaved PARP1 is associated with oocyte loss in the Msh5 null mutant ovary.
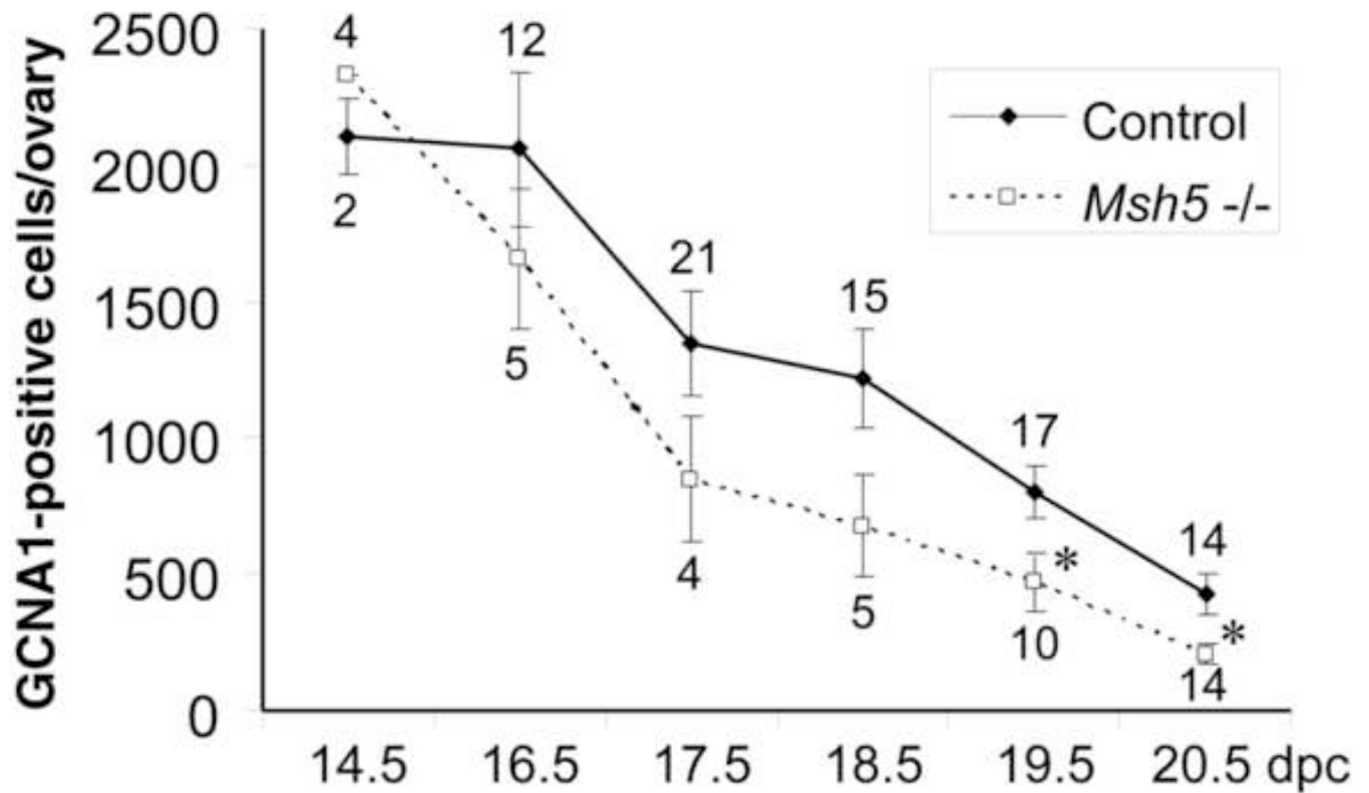
Fig. 1.
The total number of GCNA1-positive cells in *Msh5* −/− ovaries compared to the control (+/+ and +/−) ovaries at progressive developmental stages. Each value indicates the mean ± s.e.m. The number of examined ovaries is shown near the s.e.m. * Significant difference (P<0.05) compared to the control.
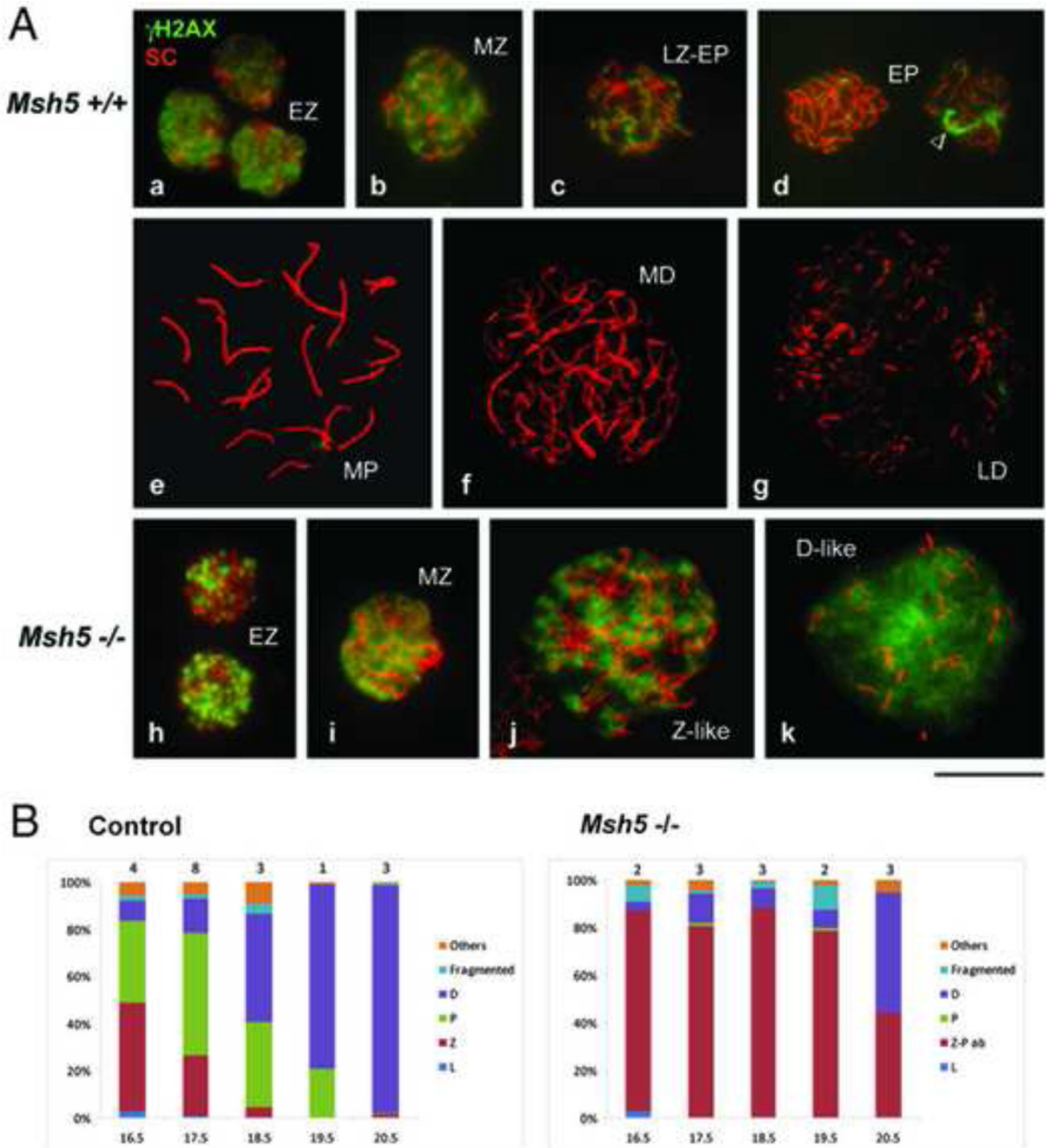
Fig. 2.
Meiotic prophase progression in oocytes during ovarian development.**A**. Typical IF staining for SC (red) and γH2AX (green) in the oocytes from *Msh5* +/+ (a–g) and *Msh5* −/− (h–k) ovaries. Bar 40 μm.
a. Early zygotene. Partial thickening of SC is seen while the entire nucleus is labeled for γH2AX. **b**. Mid zygotene. SC cores are further thickened and shortened. **c**. Late zygotene-early pachytene. The intensity of γH2AX staining decreased. **d**. Early pachytene. The staining for γH2AX has disappeared except for a few foci or intense staining along a SC core (arrowhead), which likely harbors persistent asynapsis. **e**. Mid pachytene. Discrete 20

SC cores are seen. **f**. Mid diplotene. Most homologous chromosomes are dissociated except for crossovers. **g**. Late diplotene. SC cores are thinner and fragmented. **h**. Similar to early zygotene (a). **i**. Similar to mid zygotene (b). **j**. Zygotene-like. Most chromosomes remain asynapsed and the entire nucleus is labeled for γH2AX like zygotene. However, chromosomes are spread into a large area more like pachytene. **k**. Late diplotene-like. SC cores are faint and fragmented like the normal late diplotene (g). However, the entire nucleus is labeled for γH2AX. Therefore, this nucleus can be categorized as early zygotene except for the large size.

B. Percentage of SC-positive oocytes at progressive meiotic stages from the control and *Msh5* –/– ovaries. The number of examined ovaries is given on the top of each column.
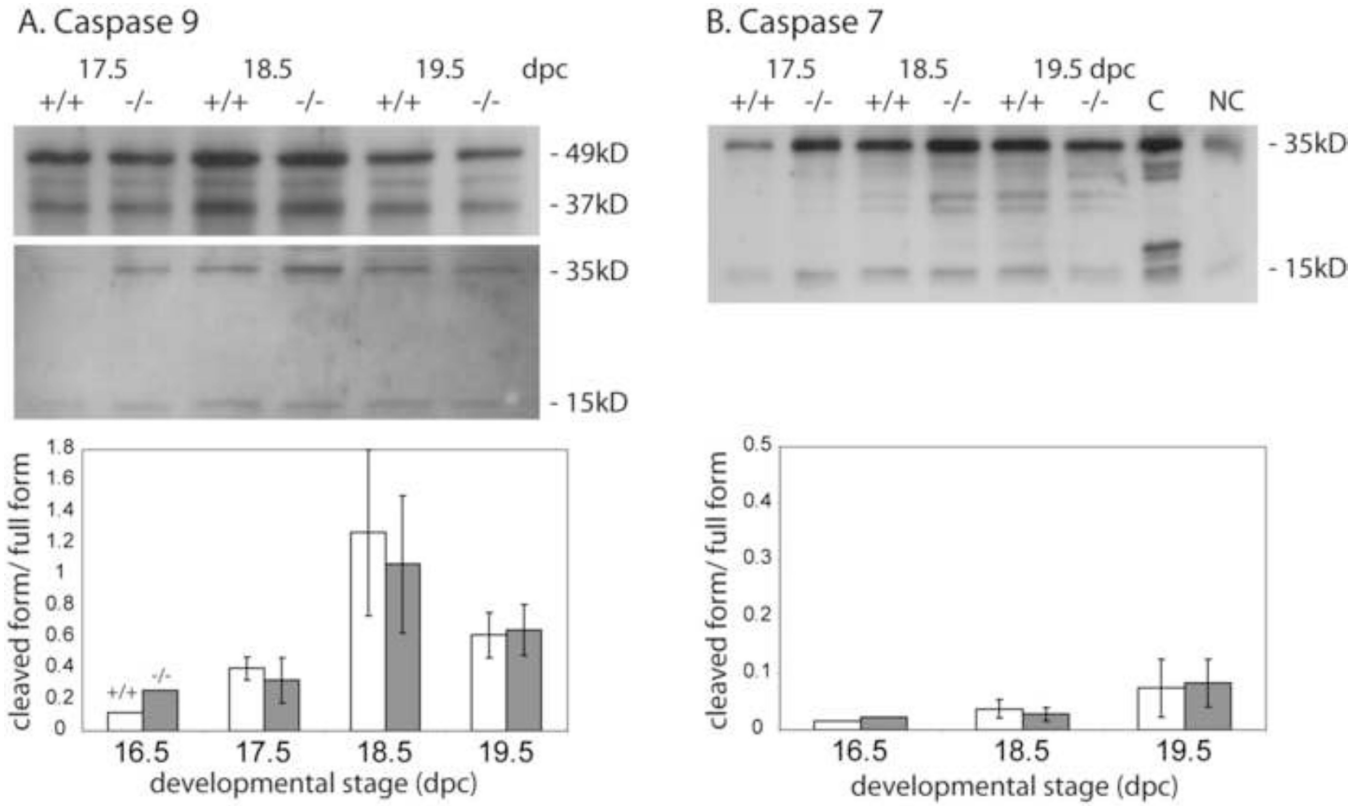
Fig. 3.
Cleavage of caspases 7 and 9 in *Msh5* +/+ and –/– ovaries during fetal development.
A. Immunoblot of caspase 9. The antibody from Cell Signaling recognized the 49 kDa procaspase 9 and its 37 and 39 kDa cleaved forms (top) while the antibody from Imergen recognized 35 and 15 kDa cleaved forms (middle). The activation level was calculated by the ratio of 37 kDa to 49 kDa band intensities (bottom). Three sets of ovaries were examined at each developmental stage except for one set at 16.5 dpc. Each column indicates the mean ± s.e.m.
B. Immunoblot of caspase 7. The antibody recognized the 35kDa procaspase 7 and its 16 kDa cleaved form in both ovarian lysate and the positive control (C, human Jurkat cells treated with etoposide) but not in the negative control (NC, human Jurkat cells without apoptosis induction) (top). The activation level was calculated by the ratio of 16 kDa to 35 kDa band intensities (bottom). 2, 3, and 3 sets of ovaries were examined at 16.5, 18.5, and 19.5 dpc, respectively. Each column indicates the mean ± s.e.m.
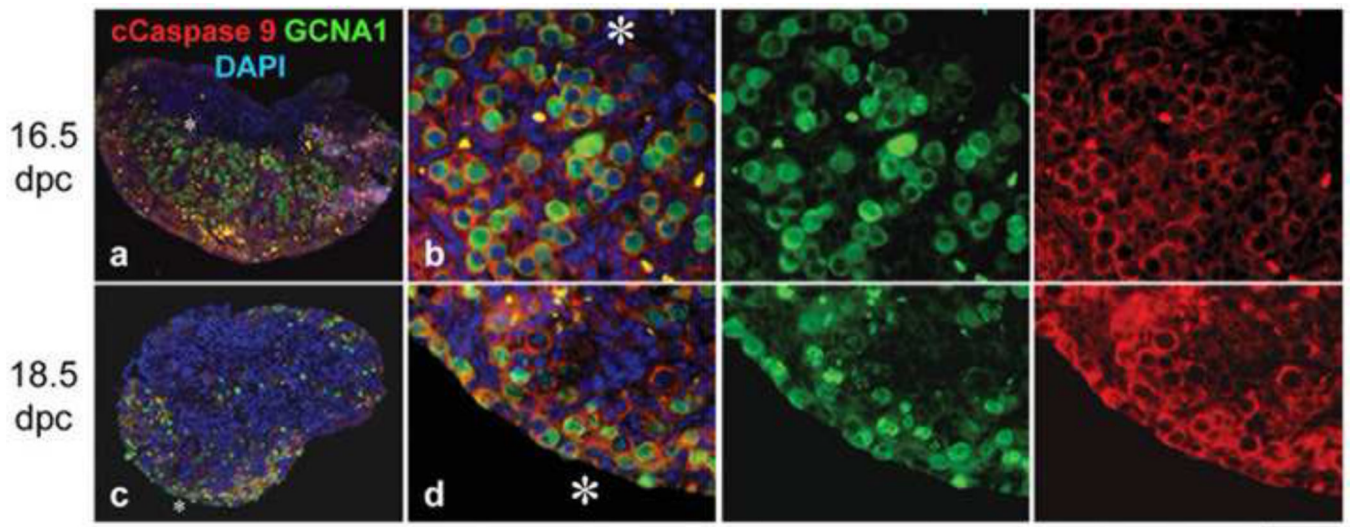
Fig. 4.
IF localization of cleaved caspase 9 in histological sections of *Msh5* +/+ ovaries. IF staining for the 15/35 kDa fragments of caspase 9 (red) and GCNA1 (green) is merged with DAPI counterstaining (blue) in **a–d**, followed by green and red signals alone. Bar 160 μm in a, c and 40 μm in b, d.
**a & b**. At 16.5 dpc. The asterisk indicates the same site of the section. The cleaved caspase 9 is distributed evenly in the cytoplasm of almost all oocytes. Yellow signals are autofluorescence in blood cells. **c & d**. At 18.5 dpc. The staining for cleaved caspase 9 is intense in the cytoplasm of some oocytes.
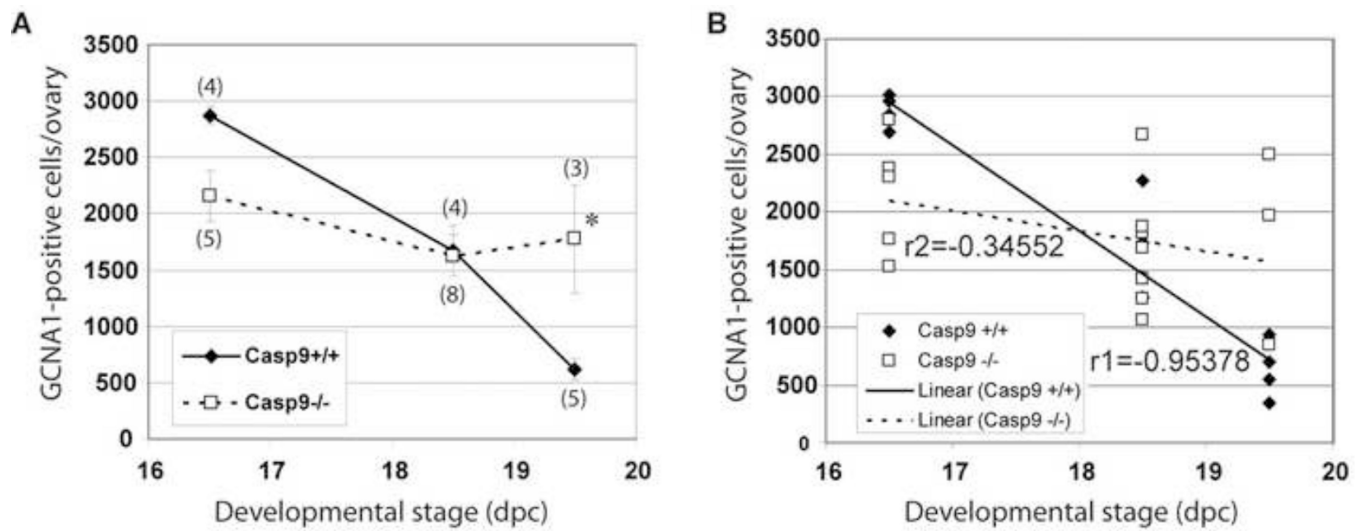
Fig. 5.
The total number of GCNA1-positive cells in *Casp9* −/− ovaries compared to *Casp9* +/+ ovaries at progressive developmental stages.

- **A.** Each value indicates the mean ± s.e.m. The number of examined ovaries is shown in parentheses. * denotes significant difference (P<0.05) by student t-test.

- **B.** Regression analysis indicates a significant difference (P<0.001) between the rate of oocyte loss in Casp9 +/+ and −/− ovaries.
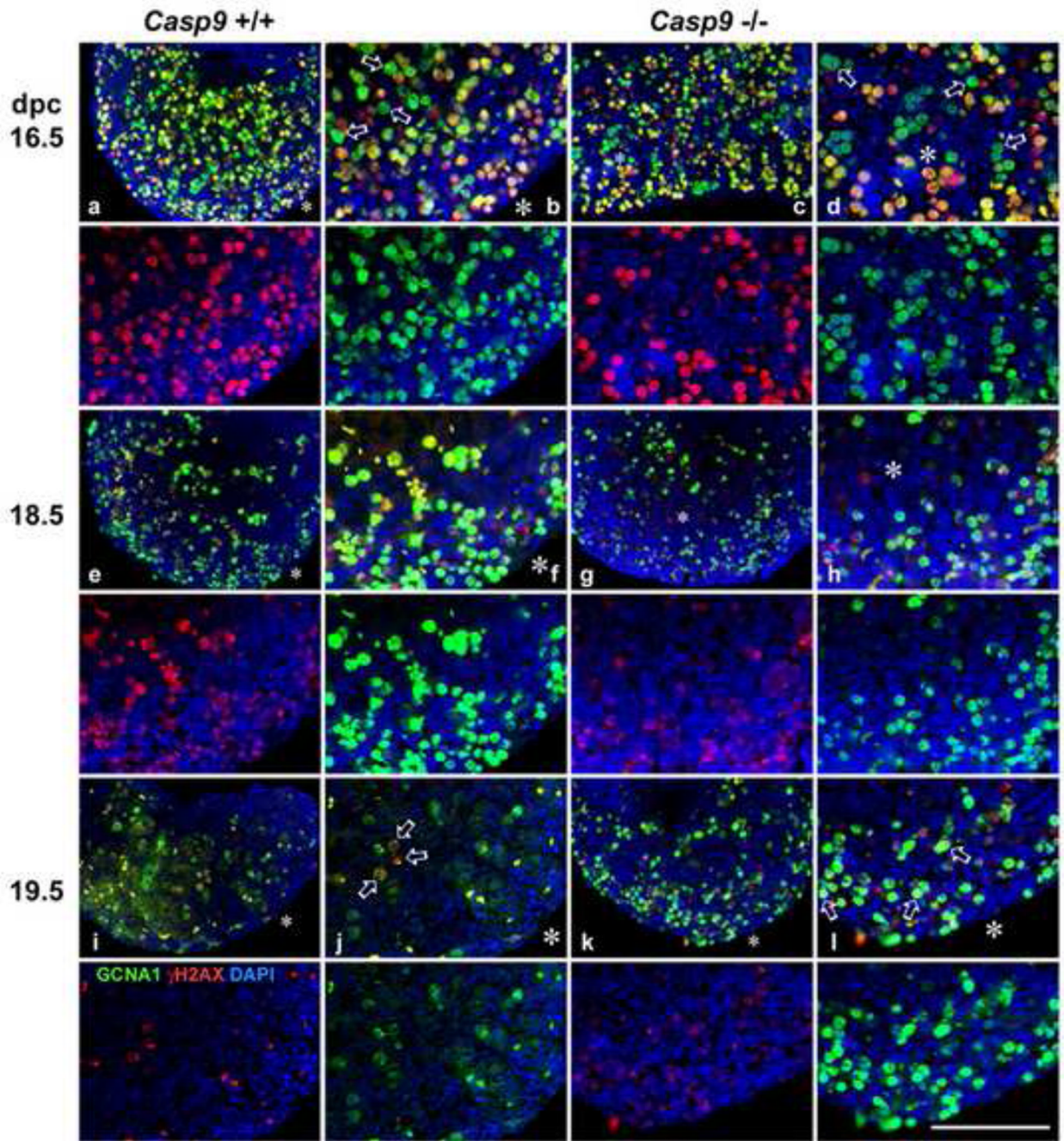
Fig. 6.
Distribution and meiotic stages of oocytes in *Caps9* +/+ (left) and −/− (right) ovaries at progressive developmental stages. IF staining for GCNA1 (green) and γH2AX (red) was merged with DAPI counterstaining (blue). **a, c, e, g, i, k**. At a low magnification with overlays. **b, d, f, h, j, l**. At a higher magnification with overlays, followed by red and green signals alone underneath. * indicates the same site of a section in the two corresponding pictures. Bar 50 and 25 μm at low and high magnifications, respectively.
a–d. At 16.5 dpc. Numerous germ cells were heavily labeled for γH2AX, indicating that the vast majority of oocytes are at the leptotene to zygotene stages. Some GCNA1-positive cells

(arrows) are γH2AX-negative, indicating that DSBs have not yet been formed in these cells. **e–h**. At 18.5 dpc. A smaller number of GCNA1-positive cells are seen, most of which show fine γH2AX foci, indicating that they have progressed to the late zygotene to early pachytene stages. **i & j**. *Caps9* +/+ ovary at 19.5 dpc. The number of GCNA1-positive cells has further decreased. Most oocytes have no or few γH2AX foci, characteristics of the late meiotic prophase except for a few (arrows) with many yH2AX foci. **k & l**. *Caps9* –/– ovary at 19.5 dpc. For comparison with the *Caps9* +/+ ovary, a greater number of GCNA1-positive cells are seen. Their majority show many fine γH2AX foci, characteristics of the late zygotene to early pachytene stages. Some oocytes (arrowheads) are γH2AX-negative, characteristic of the late meiotic prophase.
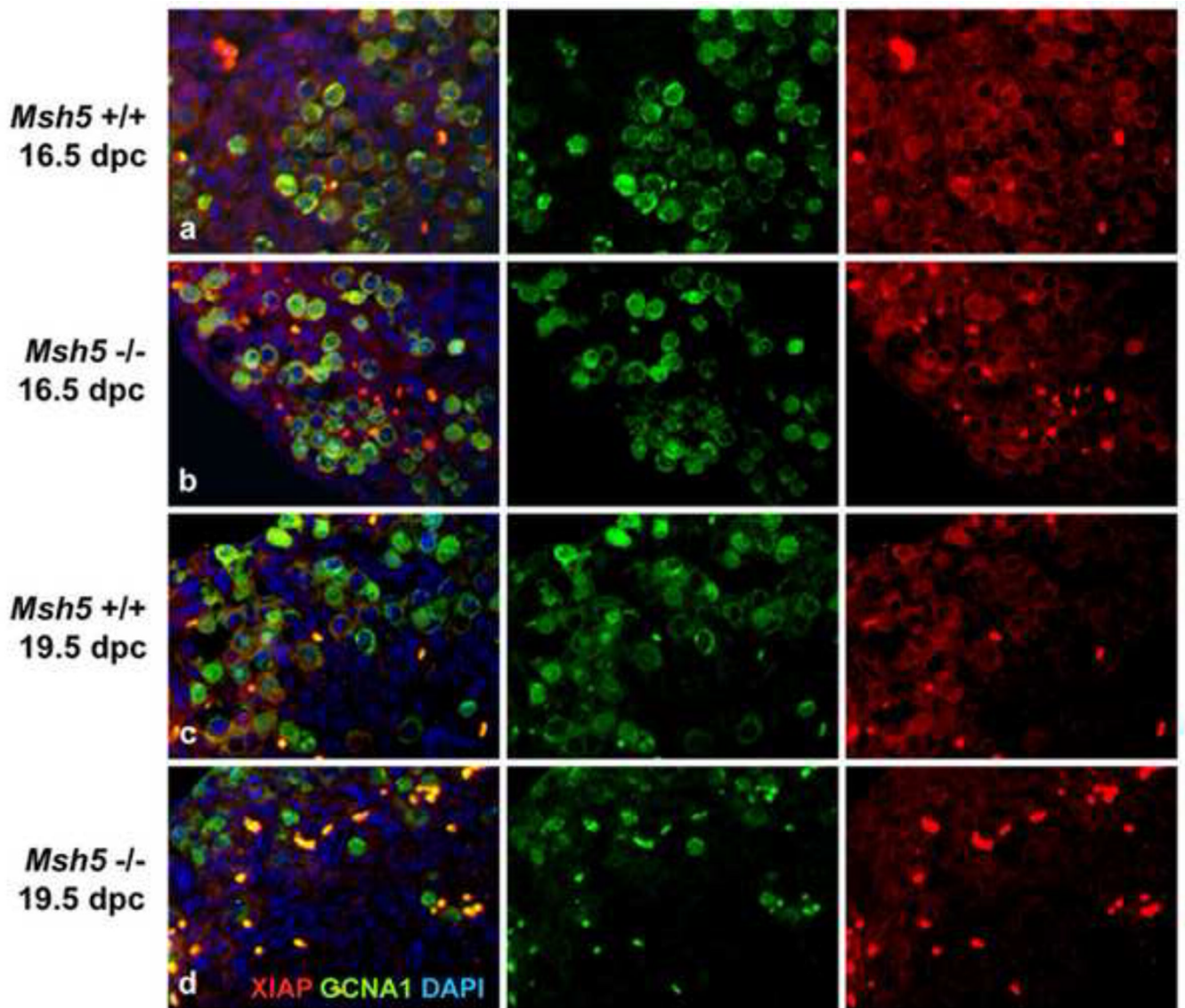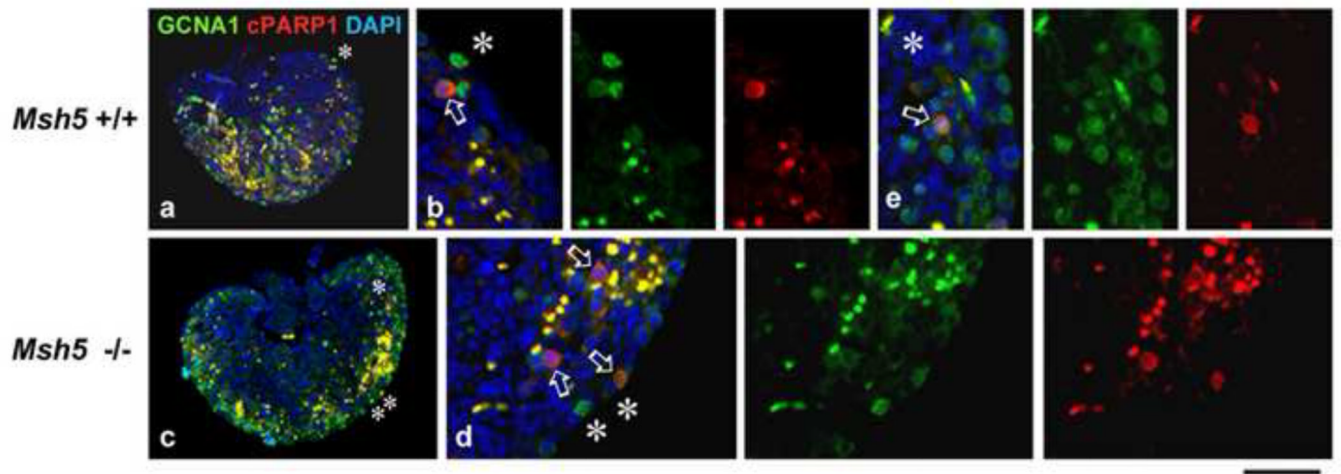
Fig. 7.
IF localization of XIAP in *Msh5* +/+ and −/− ovaries at 16.5 and 19.5 dpc. IF staining for XIAP (red) and GCNA1 (green) is merged with DAPI counterstaining in **a–d**, followed by green and red signals alone. Bar 40 μm.
a. *Msh5* +/+ ovary at 16.5 dpc. XIAP staining is seen in the cytoplasm of almost all oocytes. **b**. *Msh5* −/− ovary at 16.5 dpc. Similar to the *Msh5* +/+ ovary (a). **c**. *Msh5* +/+ ovary at 19.5 dpc. XIAP staining in the cytoplasm is more irregular compared to the ovary at 16.5 dpc. **d**. *Msh5* −/− ovary at 19.5 dpc. XIAP staining in the cytoplasm is less intense compared to the *Msh5* +/+ ovary (c) or the *Msh* −/− ovary at 16.5 dpc (b).

Fig. 8.
IF localization of cleaved PARP1 in *Msh5* +/+ and −/− ovaries at 19.5 dpc. IF staining for the 24 kDa fragment of PARP1 (red) and GCNA1 (green) is merged with DAPI counterstaining (blue) in **a–e**, followed by green and red signals alone. Bar 160 μm in a, c and 40 μm in b, d, e.
a & b. *Msh5* +/+ ovary. The arterisk indicates the same site of the section. One oocyte (arrow) is double labeled for GCNA1 and cPARP1. **c–e**. *Msh5* −/− ovary. The single and double asterisks indicate the same sites of the section. A few oocytes (arrows) are double labeled for GCNA1 and cPARP1.
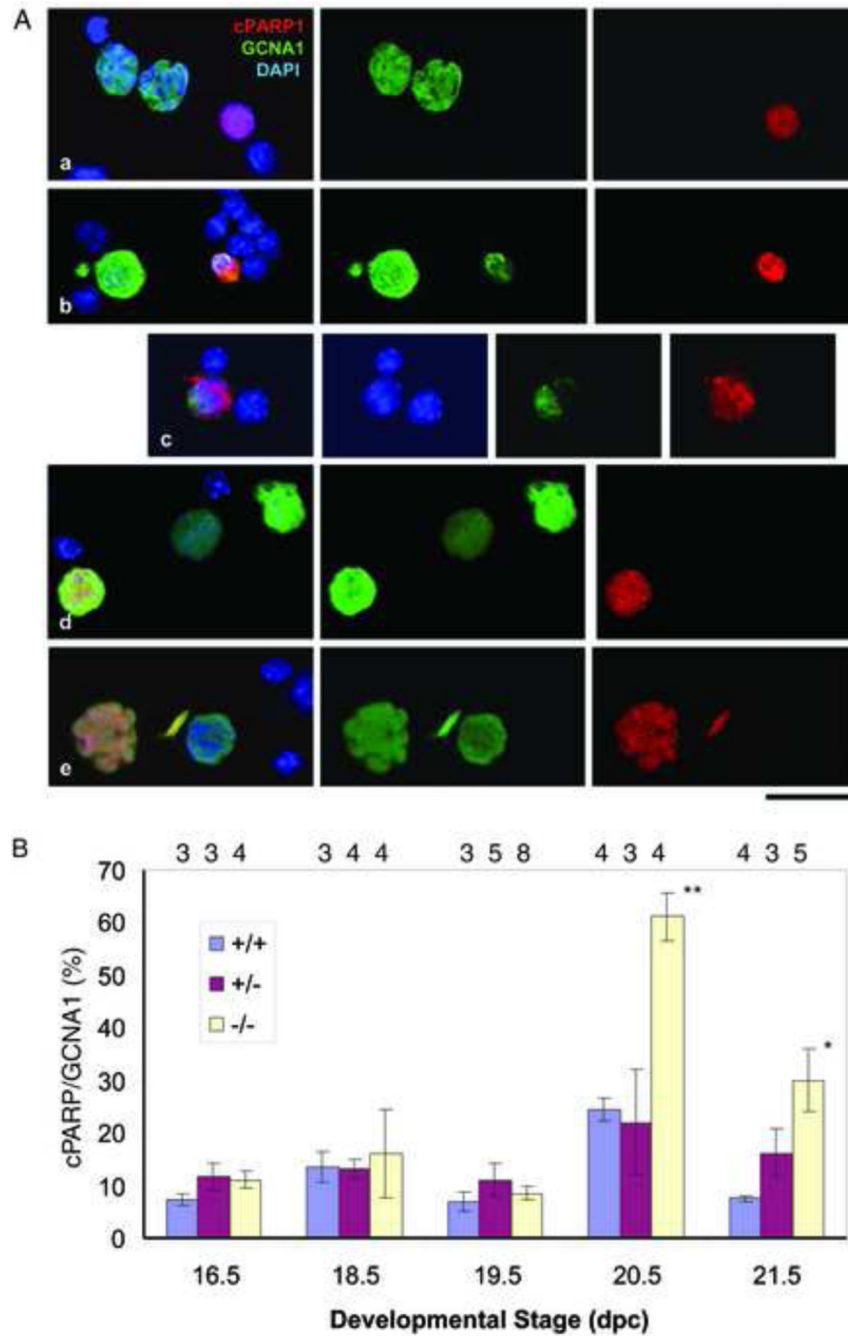
Fig. 9.
Frequency of cPARP1-positive germ cells in the dissociated cell preparations from *Msh5* +/
+, +/−, and −/− ovaries at progressive developmental stages.
A. Variable patterns of IF staining for cPARP1 (red) and GCNA1 (green) merged with
DAPI counterstaining (blue), followed by green and red signals alone except that DAPI
signals alone are also shown in c. Bar 40 μm.
a. The entire nucleus of one oocyte is labeled for cPARP1. GCNA1 staining indicates
condensed chromosomes, typical of the mid meiotic prophase. Another oocyte nearby is
negative for cPARP1. **b**. The entire nucleus of one oocyte is labeled for cPARP1 while other

oocyte nuclei are negative. **c**. GCNA1 staining is seen only in half of the nucleus while cPARP staining covers the entire nucleus. **d**. The nucleus labeled for both GCNA1 and cPARP1 is considerably smaller than the typical oocyte nucleus nearby, which is cPARP1-negative.

B. Percentage of cPARP1-positive cells among GCNA1-positive cells. Each column indicates the mean ± s.e.m. The number of examined ovaries is given on the top of each column. ** and * indicate statistical differences from either *Msh5* +/+ or *Msh5* +/− ovaries by ANOVA (P<0.01 and 0.05, respectively).